Electronic Supplementary Material (ESI) for RSC Advances.

Supplementary Information

High chlorine evolution performance of electrochemically reduced TiO_2 nanotube array coated with thin RuO_2 layer by the self-synthetic method

Teayoung Lee [a], Woonghee Lee [b], Seongsoo Kim[a], Changha Lee[a], Kangwoo Cho[b], Choonsoo Kim[c,*], and Jeyong Yoon[a,d,*]

[A.] School of Chemical and Biological Engineering, Institute of Chemical Processes (ICP), Seoul National University, 1 Gwanak-ro, Gwanak-gu, Seoul 08826, Republic of Korea e-mail: jeyong@snu.ac.kr
[b.] Division of Environmental Science & Engineering, POSTECH, 77 Chungam-ro, Nam-gu, Pohang 37673, Republic of Korea
[c.] Department of Environmental Engineering and Institute of Energy/Environment Convergence Technologies, Kongju National University,1223-24, Cheonan-daero, Cheonan-si 31080, Republic of Korea, e-mail: choonsoo@kongju.ac.kr
[d.] Korea Environment Institute, 370 Sicheong-daero, Sejong-si 30147, Republic of Korea,

[*] Corresponding author: jeyong@snu.ac.kr (J. Yoon) and choonsoo@konju.ac.kr (C. Kim)

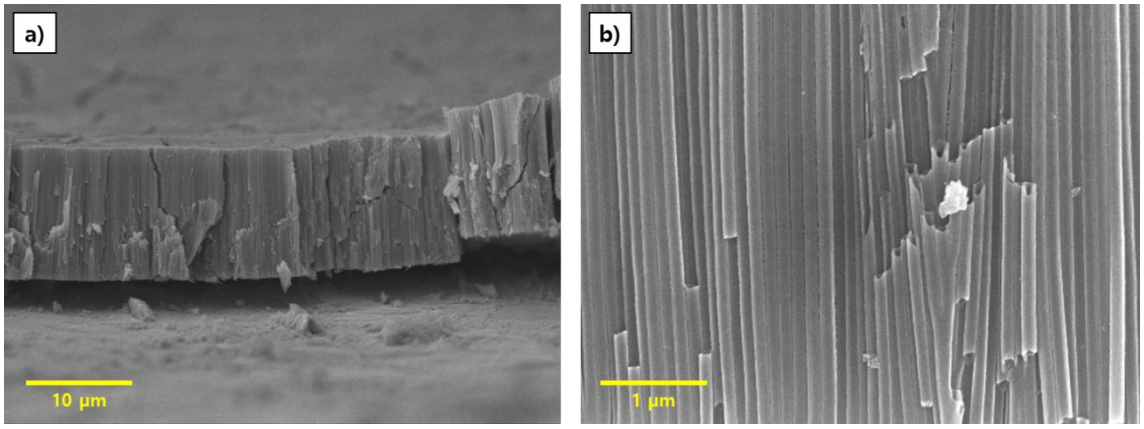

Figure S1. Field emission scanning electron microscope (FE-SEM) images (cross sectional view) for a) the thickness and b) the width of prepared TiO_2 nanotube array after the second anodization for 7 h in 40 V

The prepared TiO_2 nanotube array (TiO_2 NTA) has the thickness of ~ 13.8 µm, and the width of nanotubes was around 130±30 nm in Fig. S1. The TiO_2 NTA were electrochemically reduced (r-TiO_2), and it was employed for coating RuO_2 on the surface (RuO_2@TiO_2).

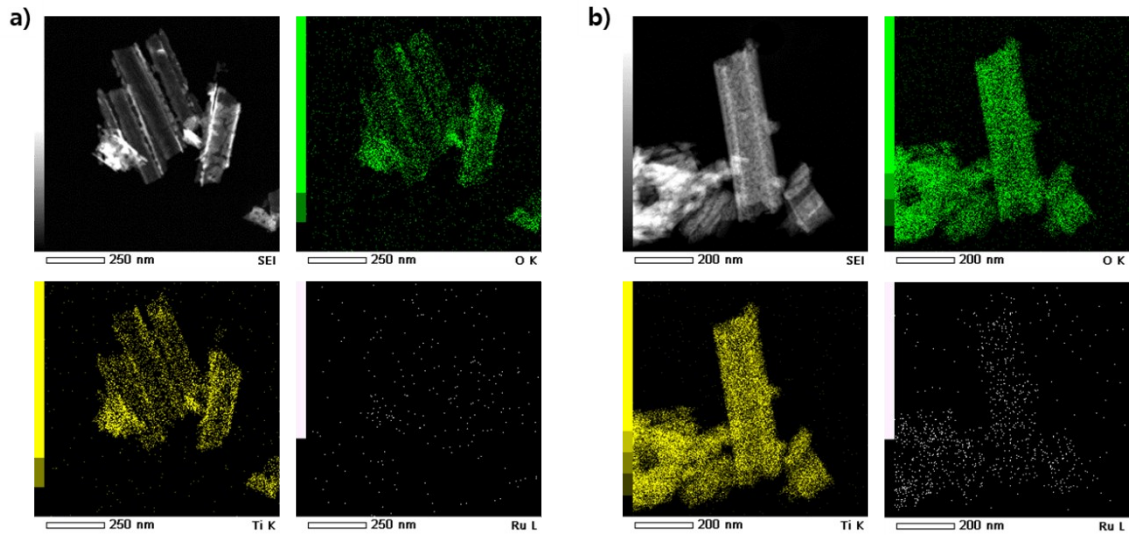

Figure S2. Energy-dispersive X-ray spectroscopy (EDS) of the field emission electron microscope (FE-TEM); a) r-TiO_2 and b) RuO_2@TiO_2 (green: oxygen, yellow: titanium, white: ruthenium)

In order to confirm the deposits based on ruthenium after coating RuO_2 on r-TiO_2 (RuO_2@r-TiO_2), an energy-dispersive X-ray spectroscopy (EDS) of a field emission transmission electron microscope (FE-TEM) was employed. As shown in Fig. S2, titanium (yellow) and oxygen (green) were detected evenly on both r-TiO_2 and RuO_2@r-TiO_2. Note that the Ru signal in EDS is weaker than Ti. It can be explained by that the structural density of r-TiO_2 and RuO_2. The structure of r-TiO_2 can be highly dense since the nanotube is formed by anodization of Ti plate whereas the RuO_2 thin layer was grown from Ru metal seed with self-oxidation of Ti(III) leading to a less dense structure. However, only RuO_2@r-TiO_2 had the ruthenium (white) along to the shape. In this regard, the ruthenium related material was coated successfully on the overall r-TiO_2, but it was not able to be the key evidence of RuO_2 coating because the detection of oxygen was inevitable from TiO_2.

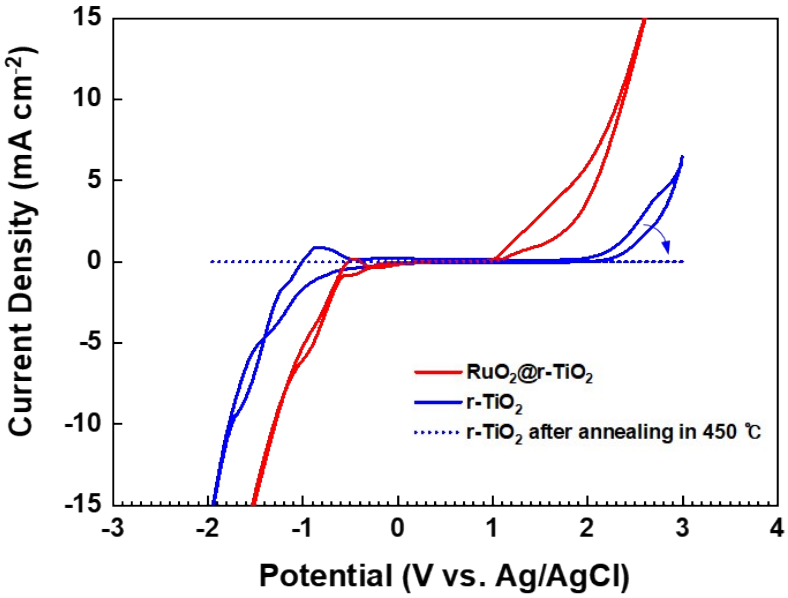

Figure S3. Cyclic voltammograms (CVs) of RuO_2@r-TiO_2, r-TiO_2, and r-TiO_2 after annealing in 450 ℃; 0.1 M phosphate buffer solution (PBS), 5 mV s^{-1}, Ag/AgCl (in sat. KCl) reference electrode. Note that the CVs of RuO_2@r-TiO_2 and r-TiO_2 were from Fig. 5a to show the effect of the thermal treatment.

As shown in Fig. S3, the electrochemical property of r-TiO_2 was vanished after annealing in 450 ℃ and air condition (blue arrow). It seems that the reduced surface of r-TiO_2 was oxidized on the thermal treatment. As investigated in XPS results (Fig. 4b-d), RuO_2 was formed on the RuO_2@r-TiO_2 and it took a key role for enhancing the anodic reaction (oxygen evolution reaction; OER) without losing the electrochemical properties of r-TiO_2 under thin RuO_2 layer. It implies that the self-synthesized thin layer prevented to lose the electrochemical property of the r-TiO_2 in the annealing condition and the formed RuO_2 on r-TiO_2 was a pivotal factor to improve electro-catalytic activity of RuO_2@r-TiO_2.

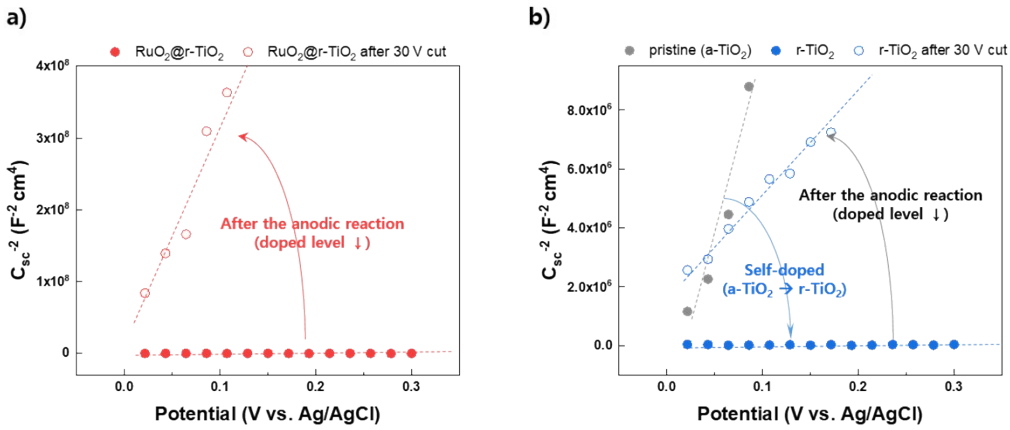

Figure S4. Mott-Schottky plot of a) RuO_2@r-TiO_2 and b) r-TiO_2 obtained with the stability tests. The Mott-Schottky plot was obtained with AC potential of 10 mV (frequency = 100 Hz) and DC potential of open circuit potential in 0.1 M KH_2PO_4 (PBS) with NaOH (pH of 7.2). The anodic reaction was conducted in the same condition as the lifetime test (Fig. 5b; 16.7 mA cm^{-2}, 0.1 M PBS).

Fig. S4 shows the Mott-Schottky plot of r-TiO_2 and RuO_2@r-TiO_2 to examine their mechanism of performance degradation. As can be seen in Fig. S4a, with long-term anodic reaction, a significant increase in slope of Mott-Schottky was found. Since the inverse the slope of Mott-Schottky means the doping level (i.e., the amount of Ti(III)), we see the doping level of RuO_2@r-TiO_2 was notably decreased during the anodic reaction. It may be attributed to that the Ti(III) on r-TiO_2, which is produced by an electrochemical reduction in the crystal lattice of a-TiO_2 NTA, is oxidized to Ti(IV) in an anodic environment leading to the non-metallic characteristics of the surface of r-TiO_2. This is well supported by the slope increase in Mott-Schottky plot of r-TiO_2 during the anodic reaction (Fig. S4b). Considering the trend of slope increase of r-TiO_2 is in good agreement with the result of RuO_2@r-TiO_2 (Fig. S4a), it is plausible that the doping level of r-TiO_2 is a fundamental factor for the degradation mechanism.

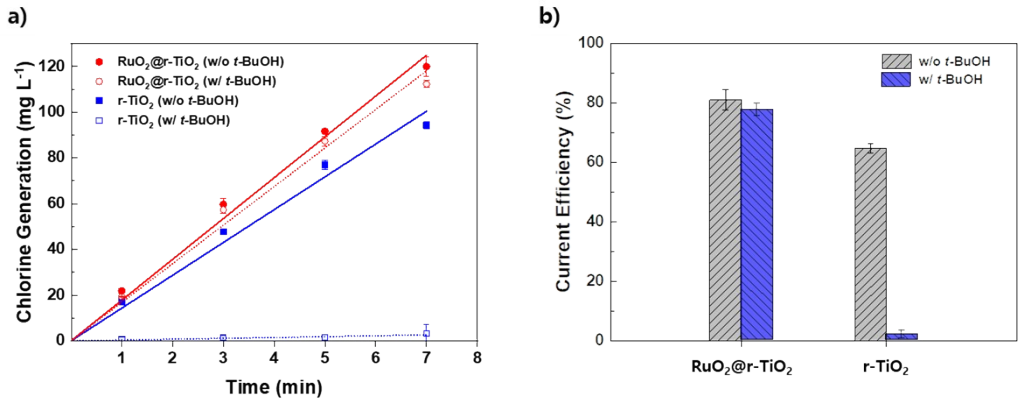

Figure S5. a) Evolution of chlorine (16.7 mA cm^{-2}, 0.1 M NaCl without and with 1M *t*-butanol (*t*-BuOH) as a hydroxyl radical scavenger) and b) The current efficiency of electrodes (RuO_2@r-TiO_2 and r-TiO_2) with and without 1 M *t*-butanol (*t*-BuOH) in 16.7 mA cm^{-2}, 3 min, 0.1 M NaCl. Note that the chlorine evolution and its efficiency without *t*-BuOH were from Fig. 6a comparing to with *t*-BuOH.

Each anode has its specific pathway for chlorine evolution reaction (ClER). RuO_2 is one of well-known materials as an active anode. On the other hand, r-TiO_2 is one of inactive materials and produces the chlorine via OH radical as an intermediate on the surface. In regard this, it is necessary that the ClER of r-TiO_2 would be limited in the OH radical scavenger (*t*-butanol; *t*-BuOH) as shown in Fig. S5. The chlorine generation of r-TiO_2 was obstructed by the *t*-BuOH which scavenges hydroxyl radicals (blue dash line), and the rate (the current efficiency) decreased from 14.35 (64.7%) to 0.37 (1.9% in Fig. S4b) mg L^{-1} min^{-1}. In contrast, the rate (the current efficiency) of RuO_2@r-TiO_2 with *t*-BuOH (red dash line, 16.87 mg L^{-1} min^{-1}, 77.8% in Fig. S5) was not changed meaningfully than 17.85 mg L^{-1} min^{-1} (81.0%) of RuO_2@r-TiO_2 without *t*-BuOH. Eventually, this indicates the surface of RuO_2@r-TiO_2 was favorable to chlorine evolution than hydroxyl radical and RuO_2@r-TiO_2 followed the ClER pathway of RuO_2[2].

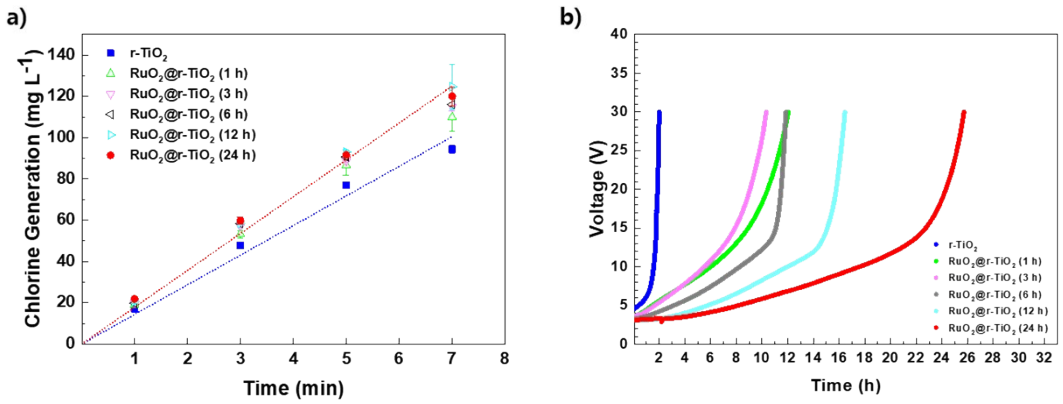

Figure S6. a) The chlorine generation in 0.1 M NaCl and b) life time test in 0.1M PBS of immersing time varied electrodes (r-TiO_2 and 1, 3, 6, 12, 24 h treated RuO_2@r-TiO_2); the applied current density 16.7 mA cm^{-2}

Fig. S6 shows the improvement of electrochemical properties in varying the immersing time in ruthenium precursor. Comparing to r-TiO_2, the chlorine generation increased even it was treated for 1 h, and it was enhanced gradually in Fig. S5a. In order to compare to each samples, the current efficiency and energy consumption were presented on Fig. 8b.

The stabilities of each electrode were conducted in 0.1 M phosphate buffer solution (PBS) and a constant current of 16.7 mA cm^{-2}. According to the immersing time in ruthenium precursor, the stability increased up to ~22 h (Fig. S6b). Note that the stabilities of each samples were able to be measured with the time at the substantial increase of the voltage.

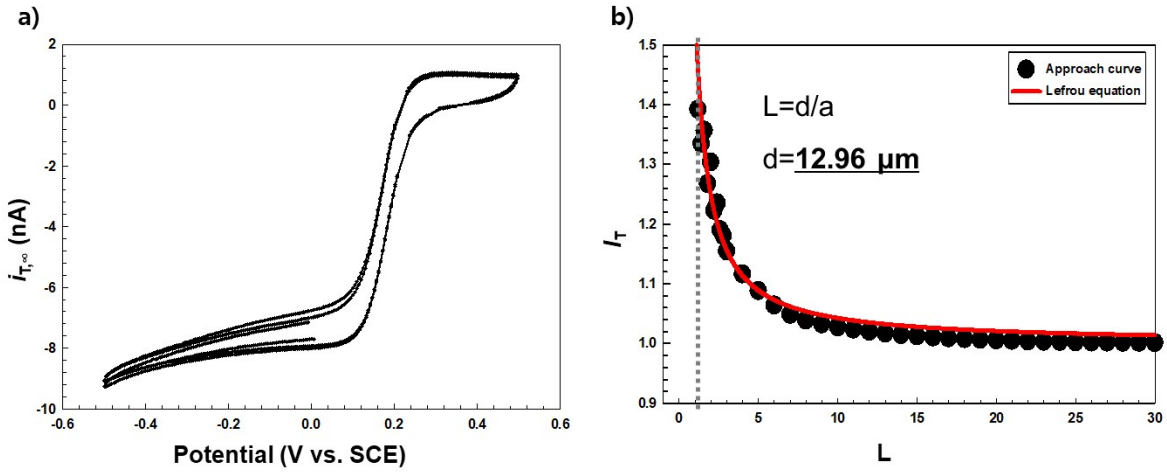

Figure S7. a) CV for stabilizing Pt tip in 5 mM $K_3Fe(CN)_6$ with 0.1 M KCl and b) approach curve for determination of the distance between tip and sample; a: tip diameter of 10 µm, d: the distance of tip-to-sample

A sample generation/tip collection (SG/TC) mode of SECM[3,4] was employed to scrutinize activity for ClER on RuO_2 coated sample, without an effect of iR-drop and double layer charging current[3]. The activity for ClER could be directly visualized by scanning along with sample, which is called as area scan. Before the area scan, it is necessary to calculate distance between tip and sample and detect reduction potential of chlorine at the tip as well.

M470 SECM workstation and SP-300 Bipotnetiostat (Biologic Science Instruments SAS, France) were used for an area scan and a Pt ultra-microelectrode (UME) tip with diameter of 10 µm (RG ratio = 10) was also provided by BioLogic. The Tip was activated until reproducible cyclic voltammograms and rinsed with deionized water before using.

Firstly, in Fig. S7a, Pt tip was stabilized in 5 mM $K_3Fe(CN)_6$ with 0.1 M KCl (Alfa Aesar, USA), and then a distance between sample and tip, 12.96 µm, was calculated from the approach curve in Fig. S7b. The tip current (I_T) was augmented by the positive feedback, corresponding to re-oxidization of redox mediator, Fe^{2+}, on the conductive sample.

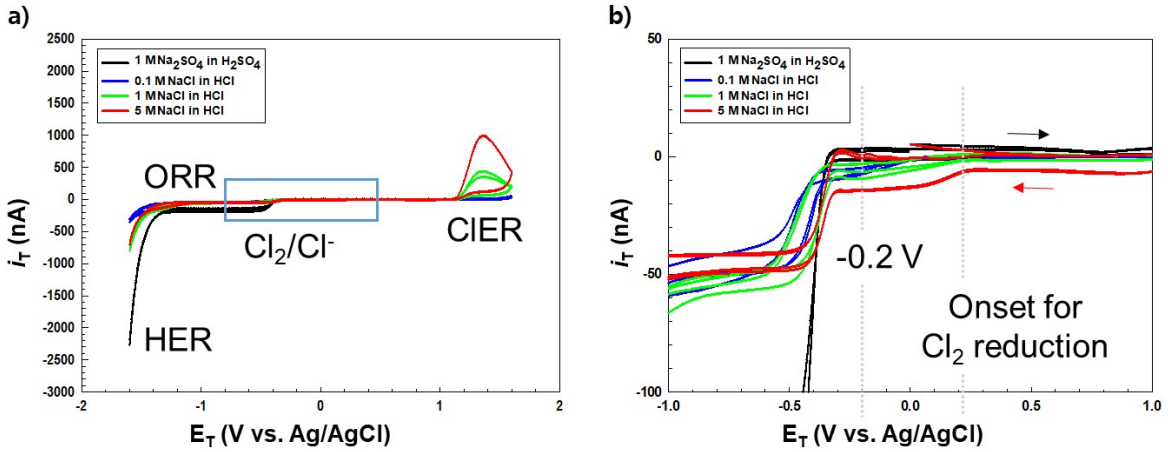

Figure S8. a) Comparison of CVs in the presence of chloride (Cl^-) with various concentrations (0, 0.1, 1, 5 M) and b) enlarged CVs for detecting reduction potential of chlorine (Cl_2) at the tip (scan rate of 50 mV s^{-1}, tip diameter of 10 μm, pH 2)

As shown in Fig. S8, the potential of chlorine reduction reaction (ClRR) was observed that the steady-state current for chlorine reduction at tip in acidic media (pH 2) was clearly detected at -0.2 V vs. Ag/AgCl during the chlorine generation on the sample at the same time. In comparison, oxygen reduction reaction (ORR) was marked in Na_2SO_4 adjusted to pH 2. Accordingly, the tip potential was set to be -0.2 V vs. Ag/AgCl for detecting reduction of chlorine in the area scan.

References

1. C. Kim, S. Kim, J. Choi, J. Lee, J.S. Kang, Y.E. Sung, J. Lee, W. Choi, J. Yoon, Blue TiO_2 nanotube array as an oxidant generating novel anode material fabricated by simple cathodic polarization, Electrochim. Acta. 141 (2014) 113–119.

2. Kim, C. Kim, S. Kim, J. Yoon, RuO_2 coated blue TiO_2 nanotube array (blue TNA-RuO_2) as an effective anode material in electrochemical chlorine generation, J. Ind. Eng. Chem. 66 (2018) 478–483.

3. . Zeradjanin, T. Schilling, S. Seisel, M. Bron, W. Schuhmann, Visualization of chlorine evolution at dimensionally stable anodes by means of scanning electrochemical microscopy, Anal. Chem. 83 (2011) 7645–7650.

4. Bard, A. J., Faulkner, Electrochemical Method: Fundamental and Applications, 2nd ed., John Wiley & Sons, Inc., New York, 2001.